



Mechanical and Aerospace Engineering

Box 876106

Tempe, Arizona 85287-6106

Professor William S. Saric

480-965-2822

FAX: 480-965-1384

E-mail: saric@asu.edu

<http://wtsun.eas.asu.edu>

We are pleased to provide you a complimentary copy of our Annual Reviews article as a PDF file for your own personal use. Any further/multiple distribution, publication or commercial usage of this copyrighted material would require submission of a permission request addressed to the Annual Reviews Permissions Department, email permissions@AnnualReviews.org

BOUNDARY-LAYER RECEPTIVITY TO FREESTREAM DISTURBANCES

William S. Saric¹, Helen L. Reed¹, and Edward J. Kerschen²

¹*Mechanical and Aerospace Engineering, Arizona State University, Tempe, Arizona 85287-6106; e-mail: saric@asu.edu, helen.reed@asu.edu*

²*Aerospace and Mechanical Engineering, University of Arizona, Tucson, Arizona 85721-0119; e-mail: kerschen@ame.arizona.edu*

Key Words sound, stability, transition, turbulence

■ **Abstract** The current understanding of boundary-layer receptivity to external acoustic and vortical disturbances is reviewed. Recent advances in theoretical modeling, numerical simulations, and experiments are discussed. It is shown that aspects of the theory have been validated and that the mechanisms by which freestream disturbances provide the initial conditions for unstable waves are better understood. Challenges remain, however, particularly with respect to freestream turbulence.

1. INTRODUCTION

Establishing the origins of turbulent flow and transition from laminar to turbulent flow remains an important challenge for fluid mechanics. The common thread connecting aerodynamic applications is the fact that they deal with bounded shear flows (boundary layers) in open systems (with different upstream or initial amplitude conditions). It is well known that the stability, transition, and turbulent characteristics of bounded shear layers are fundamentally different from those of free shear layers (Morkovin 1969, Reshotko 1976, Bayley et al. 1988). Likewise, open systems are fundamentally different from closed systems. The distinctions are trenchant and thus form separate areas of study.

At the present time, no mathematical model exists that can predict the transition Reynolds number on a flat plate. One obvious reason for this is the variety of influences such as freestream turbulence, surface roughness, sound, etc. which are incompletely understood. Reshotko (1997) gave a historical perspective of the progress and issues in transition prediction. Reed et al. (1996) reviewed the linear-stability literature and discussed the importance of this work as it relates to transition and aircraft skin-friction reduction. With the maturation of linear-stability methods and the conclusions that breakdown mechanisms are initial-condition dependent (Saric & Thomas 1984, Singer et al. 1989, Corke 1990), more

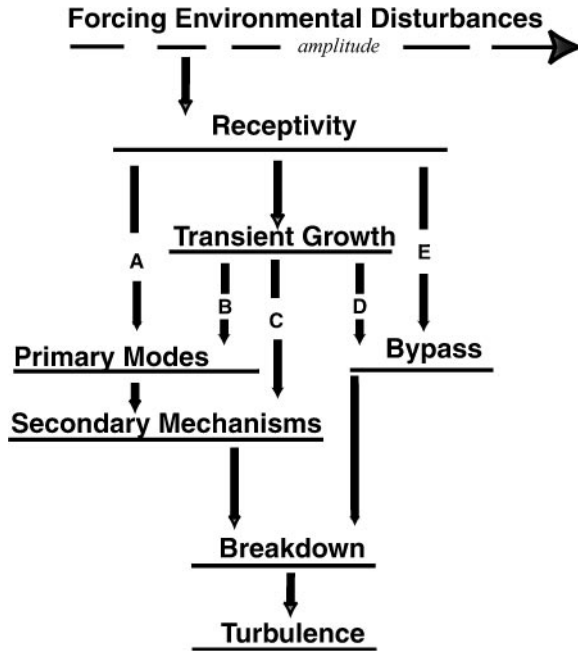


Figure 1 The paths from receptivity to transition.

emphasis is now placed on the understanding of the source of initial disturbances than on the details of the later stages of transition.

1.1. Boundary-Layer Transition

The process of transition for boundary layers in external flows can be qualitatively described using Figure 1 and the following (albeit, oversimplified) scenario based on one of the different “roadmaps” to turbulence developed over the years (Morkovin et al. 1994).

Disturbances in the freestream, such as sound or vorticity, enter the boundary layer as steady and/or unsteady fluctuations of the basic state. This part of the process is called receptivity (Morkovin 1969), and it establishes the initial conditions of disturbance amplitude, frequency, and phase for the breakdown of laminar flow. In Figure 1, the initial amplitude increases schematically from left to right. Initially these disturbances may be too small to measure, and they are observed only after the onset of an instability. A number of different instabilities can occur independently or together and the appearance of any particular type of instability depends on Reynolds number, wall curvature, sweep, roughness, and initial conditions. If Figure 1 is entered with weak disturbances and path A is followed,

the initial growth of these disturbances is described by linear stability theory of primary modes (i.e., linearized unsteady Navier-Stokes). This growth is weak, occurs over a long streamwise length scale, and can be modulated by pressure gradients, surface mass transfer, temperature gradients, etc. As the amplitude grows, three-dimensional and nonlinear interactions occur in the form of secondary instabilities. Disturbance growth is very rapid in this stage (now over a convective length scale), and breakdown to turbulence occurs.

Because the linear stability behavior can be calculated, transition prediction schemes often assume that transition follows path *A* and consider only the linear regime. This is justified on the assumption that external flows typically have weak freestream disturbances and the streamwise extent of the linear growth region is large compared to that of the nonlinear region. However, because the initial conditions (receptivity) are not generally known, only correlations between two systems with similar environmental conditions are possible. Recent critical reviews of these methods are found in Arnal (1994) and Reed et al. (1996).

At times, the freestream disturbances are so strong that the growth of linear disturbances is bypassed (Morkovin 1969, 1993) and turbulent spots or subcritical instabilities occur and the flow quickly becomes turbulent. This corresponds to path *E* in Figure 1, and although the phenomenon is not well understood, it has been documented in cases of roughness and high freestream turbulence (Reshotko 1984, 1994, 2001). In this case, transition prediction schemes based on linear theory fail completely.

It is generally accepted that bypass refers to a transition process whose initial growth is not described by the primary modes of the Orr-Sommerfeld equation (OSE). Historically, one had either path *A* or *E* from which to choose as the road to turbulence. Recently however, considerable work in the area of transient growth has expanded our understanding of different paths by which transition to turbulence can occur.

Transient growth occurs when two, nonorthogonal, stable modes interact, undergo algebraic growth, and then decay exponentially. Streamwise vorticity and wall-normal vorticity appear to be important. This mechanism was first elucidated by Landahl (1980) and then by Hultgren & Gustavsson (1981). The idea was used by Henningson et al. (1993) and others. Recent reviews appear in Andersson et al. (1999), Reshotko (2001), and Schmid & Henningson (2001).

Studies have shown that large amplitudes can be achieved through transient growth when the boundary layer is provided with appropriate initial conditions. Thus, the spectrum of initial conditions depends on receptivity. Returning to Figure 1, one can now say that, depending on amplitude, transient growth can lead to spanwise modulations of two-dimensional waves (path *B*), direct distortion of the basic state that leads to secondary or subcritical instabilities (path *C*), or direct bypass (path *D*).

In spite of progress, an overall theory remains rather incomplete with regard to predicting transition. Amplitude and spectral characteristics of the disturbances

inside the laminar viscous layer strongly influence which type of transition occurs. Thus, it is necessary to understand how freestream disturbances are entrained into the boundary layer and create the initial amplitudes of unstable waves, i.e., to answer the question of receptivity.

For this discussion, the wave instability is assumed to be of the Tollmien-Schlichting (T-S) type in two-dimensional boundary layers and the ultimate goal is to determine how the wave amplitude within the boundary layer can be found from a freestream measurement. Even though the restriction to T-S waves may make this goal seem too modest, one soon finds sufficient challenges. Because receptivity deals with the generation rather than the evolution of instability waves in a boundary layer, neither departures from the linear-mode scenario nor details of the transition process itself are discussed here.

1.2. Receptivity Processes

For incompressible flows, receptivity has many different paths through which to introduce a disturbance into the boundary layer. These include the interaction of freestream sound or turbulence with leading-edge curvature, discontinuities in surface curvature, or surface inhomogeneities. Moreover, the picture for three-dimensional flows is expected to be different than that of two-dimensional flows. Essentially, the incoming freestream disturbance at wavenumber α_{fs} interacts with an inhomogeneity of the body causing its spectrum to broaden to include the response wavenumber α_{TS} . Small initial amplitudes of the disturbances tend to excite the linear normal modes of the boundary layer that are of the T-S type (Mack 1984).

It is believed that the vortical parts of the freestream disturbances (turbulence) contribute to the three-dimensional aspects of the breakdown process (Kendall 1984, 1998), whereas the irrotational parts of the freestream disturbances (sound) contribute to the initial amplitudes of the two-dimensional T-S waves (Kosorygin et al. 1995). Thus, freestream sound and turbulence present a different set of problems in the understanding, prediction, and control of boundary transition and, as such, each requires different experimental and computational techniques.

Goldstein & Hultgren (1989) and Kerschen (1989) presented earlier reviews of receptivity. Reshotko (1994), Choudhari & Streett (1994), Crouch (1994), Saric et al. (1994), and Wlezien (1994) presented unique reviews of various aspects of receptivity. Since these reviews, papers have appeared by Breuer et al. (1996), Kobayashi et al. (1995), Kato et al. (1997), and Kachanov (2000). The latter papers deal with different aspects of three-dimensional wave motion and nonlinearities and are not discussed here.

This review naturally separates into three parts. Section 2 discusses receptivity theory in which the asymptotic analyses of Goldstein (1983, 1985) have played a seminal role. This work led to all of the progress that was later achieved by DNS and experiments. Section 3 discusses recent advances in direct numerical

simulation (DNS) of the leading-edge problem. The experiments are reviewed in Section 4.

2. THEORY

It has been shown that the parallel-flow OSE is a suitable approximation for T-S instabilities in boundary layers. The basic ideas of stability theory can be found in Mack (1984), Saric (1994b), and Reed et al. (1996), and it is assumed that the reader is familiar with this theory. One allows for normal-mode solutions where α and ω are the dimensionless streamwise wavenumber and frequency, respectively. Here, spatially developing disturbances are considered so that α is complex and is given by $\alpha = \alpha_r + i\alpha_i$ and ω is real. Because the dimensional frequency is constant throughout the flow, the reduced frequency, F , is defined as

$$F = 2\pi f\nu/U_\infty^2 \times 10^6. \quad (1)$$

2.1. Receptivity Theory

Receptivity concerns the generation of instability waves, rather than their evolution. Because boundary layers are convectively unstable, an unsteady disturbance is required to generate the instability waves. This may be a naturally occurring disturbance or an artificial forcing mechanism such as a vibrating ribbon or localized suction/blowing.

For localized, unsteady forcing mechanisms such as a vibrating ribbon or wall suction/blowing, the wavenumber spectrum of the forcing function is broad. Thus, in “forced receptivity,” the input disturbance generally contains energy at the appropriate frequency-wavelength combination to directly excite an instability wave. Hence, streamwise gradients of the mean flow do not play an essential role in forced receptivity, and this phenomenon can be analyzed within the parallel-flow OSE framework. For more information on forced receptivity, see Kerschen (1989) and Kachanov (2000).

Naturally occurring freestream forcing mechanisms consist of acoustic disturbances that propagate at the speed of sound relative to the fluid and vortical disturbances that convect at the freestream speed. In contrast, instability waves have phase speeds that are a fraction of the freestream speed. Hence, the energy for naturally occurring freestream disturbances is concentrated at wavenumbers that are significantly different than the instability wavenumber. Therefore, natural receptivity mechanisms require a wavelength conversion process.

Early attempts to develop a theory for natural receptivity were based on the OSE. This approach was not successful, because the streamwise dependence of the mean flow is neglected in the OSE. Thus, the coefficients in the equation are independent of x , and the solution within the boundary layer must exhibit the same harmonic x dependence, $\exp(i\alpha_{fs}x)$, as the freestream disturbance. Essentially, the

parallel-flow approximation precludes the transfer of energy from the wavelength of the freestream disturbance to that of the instability wave. This deficiency cannot be rectified by a multiple-scales nonparallel approach, because this only allows the mean flow to vary on the long-scale variable x/L .

The crucial role of short-scale streamwise variations of the mean flow in natural receptivity processes was first elucidated by Goldstein (1983, 1985), utilizing high-Reynolds-number asymptotics. He showed that natural receptivity occurs in regions where the mean flow changes rapidly in the streamwise direction, invalidating the parallel-flow assumption of the OSE. The regions where natural receptivity occurs can be separated into two classes. The first class (Goldstein 1983) consists of body leading-edge regions, where the boundary layer is thin and growing rapidly. The second class (Goldstein 1985) contains regions farther downstream in the boundary layer, where some local feature causes the mean flow to adjust on a short streamwise length scale. Examples of such local features are short-scale wall humps or suction strips or shock/boundary-layer interactions. Receptivity to short-scale wall humps is discussed in Section 2.5.

2.2. Leading-edge Receptivity Theory

For receptivity in the leading edge region, the Reynolds number is assumed to be large so that the outer problem corresponds to the inviscid interaction of the small-amplitude freestream disturbance with the body. This inviscid interaction provides the distributions of pressure and slip velocity that drive the unsteady motion in the boundary layer. Within the boundary layer, the small parameter that appears in the analysis is an inverse of the Reynolds number based on the length scale $U_\infty/2\pi f$ for the unsteady motion, $\varepsilon_{LE} = (2\pi f v/U_\infty^2)^{1/6} \ll 1$. Goldstein (1983) showed that the asymptotic structure for the unsteady viscous motion in the boundary layer contains two distinct streamwise regions. Near the leading edge, where $x2\pi f/U_\infty = O(1)$, the motion satisfies the linearized, unsteady, boundary-layer equation (LUBLE) for two-dimensional basic states $[U(x, y), V(x, y)]$,

$$u'_t + Uu'_x + Vu'_y + u'U_x + v'U_y = -p'_x + (1/R_L)u'_{yy}. \quad (2)$$

The LUBLE contains $u'U_x$ and Vu'_y which do not appear in the OSE and are nonparallel mean-flow effects that occur on the short-scale of the unsteady disturbance. Further downstream from the leading edge, where $x2\pi f/U_\infty = O(\varepsilon_{LE}^{-2})$, a consistent approximation leads to the classical large-Reynolds-number, small-wavenumber approximation to the OSE. Goldstein examined the asymptotic matching of these two regions, and showed that the first Lam-Rott asymptotic eigenfunction of the LUBLE, with coefficient C_1 , matches onto the T-S wave that becomes unstable farther downstream in the OSE region. Hence, the amplitude of the T-S wave is linearly proportional to C_1 , which we call the theoretical leading-edge receptivity coefficient. Here, C_1 is a complex number whose amplitude and phase are related to the T-S amplitude and phase.

To find the (complex) receptivity coefficient C_1 , a numerical solution of the LUBLE is required where the equation is analytically continued into the complex plane and solved along a ray where the first eigenfunction dominates the solution. Goldstein et al. (1983) calculated the receptivity coefficient for the case of an acoustic wave propagating downstream parallel to the surface of a flat plate. Heinrich & Kerschen (1989) developed refined numerical procedures for solution of the LUBLE and extraction of the receptivity coefficient and calculated receptivity coefficients for a variety of freestream disturbance types.

The receptivity due to small-amplitude acoustic waves impinging obliquely on the leading edge of a semi-infinite flat plate is analyzed by separating the incident acoustic field into components parallel and perpendicular to the plate surface. The parallel component contributes directly to the slip velocity on the plate surface, while the perpendicular component contributes to the slip velocity via its scattering by the plate surface. Near the leading edge, this scattered component has a square root singularity corresponding to inviscid flow around the sharp edge. The receptivity coefficient in this case is (Heinrich & Kerschen 1989)

$$|C_1| = |C_{u1} \pm C_{u2}|, \quad (3)$$

where

$$C_{u1} = 0.9508 \cos(\theta) \exp(2.0552i) \quad (4a)$$

and

$$C_{u2} = 6.2M^{-1/2} \sin(\theta/2) \exp(0.483i). \quad (4b)$$

Here θ is the incidence angle of the sound wave, $M = U_\infty/c_a$ is the Mach number, and the \pm in Equation 3 applies on the upper or lower surface of the plate, respectively. Receptivity due to scattering of the normal component of the incident acoustic wave is particularly important at low Mach numbers. As an illustration, for $M = 0.1$, the receptivity coefficients on the upper surface are $|C_1| = 0.95$ and 13.9 for $\theta = 0$ and $\pi/2$, respectively.

The above results apply only for cases in which the acoustic wavelength is short compared to both the plate length and the distance to any surrounding surfaces. To address the effect of nearby surfaces, Heinrich & Kerschen (1989) analyzed the receptivity to acoustic waves traveling upstream along the upper surface of a semi-infinite flat plate centered within a channel of width H . Again, inviscid scattering at the leading edge has a significant effect on the receptivity coefficient. For $M = 0.1$, the receptivity coefficient grows rapidly with increasing channel width, reaching a maximum $|C_1| = 35$ at $2\pi fH/c_a = \pi$. It then exhibits a regular pattern of weakly damped oscillations that gradually approach the isolated plate result for large H .

Kerschen et al. (1990) considered vortical freestream disturbances interacting with the leading edge of a flat plate. The vortical gust corresponds to a sinusoidal vorticity distribution that can be interpreted as a two-dimensional model of weak freestream turbulence. The vortical gust convects with the uniform mean flow,

has no pressure fluctuations, and the velocity fluctuations are perpendicular to the wavevector. The maximum and minimum levels of receptivity are found for freestream velocity perturbations parallel and perpendicular to the plate surface, respectively. The weak receptivity levels produced by the perpendicular component of freestream velocity are rather surprising because this component produces both a singular flow field near the leading edge and a significant slip velocity in the doubly infinite plate limit far downstream. In this case, the amplitudes and phases of these various contributions lead to a high degree of cancellation. The receptivity to the vortical gust for parallel freestream velocity fluctuations is about four times that produced by a parallel acoustic wave. This may be due to the slower phase speed of the vortical gust compared to the acoustic wave.

2.3. Parabolic Leading Edges and Aerodynamic Loading

Whereas the results for the flat-plate geometry provide important insights on leading-edge receptivity, the bodies of interest for practical applications generally have parabolic or elliptical leading edges and an asymmetric mean flow owing to the presence of aerodynamic loading. To analyze the influences of body nose radius and aerodynamic loading on leading-edge receptivity, Hammerton & Kerschen (1992, 1996, 1997, 2000) extended the asymptotic theory to the case of a parabolic leading edge. The nose radius, r_n , enters the theory through a Strouhal number, $S = r_n 2\pi f / U_\infty$. In the absence of aerodynamic loading and a parallel acoustic wave, $|C_1|$ first rises slightly (as S is increased) and then falls monotonically, to 15% of the flat-plate value at $S = 0.3$. This behavior appears to be related to the favorable pressure gradient near the nose of the parabola. For obliquely incident acoustic waves, the finite nose radius weakens the influence of leading-edge scattering, although this effect still generally dominates over the receptivity from the parallel component of the acoustic wave.

Aerodynamic loading enters with the parameter, $\mu = \alpha_{eff} (2L/r_n)^{1/2}$. Here L is the airfoil chord and α_{eff} is an effective incidence angle that depends on both the camber and angle of attack of the airfoil. The introduction of modest amounts of aerodynamic loading in the leading-edge region decreases the receptivity coefficient below the values for a symmetric mean flow. However, as the aerodynamic loading is increased toward its limiting value for attached flow, a strong rise in the receptivity coefficient occurs. This behavior appears to be related to the influence of favorable and adverse pressure gradients in the region of receptivity, $\chi 2\pi f / U_\infty = O(1)$.

In applying these results to the interpretation of transition phenomena, it is important to keep in mind the definition of the leading-edge receptivity coefficient. The receptivity coefficient C_1 is the coefficient of the first Lam-Rott asymptotic eigenfunction—the precursor to the T-S wave. An attractive feature of the leading-edge receptivity coefficient is that it is independent of frequency, f . Hence, the results presented above are applicable to all frequencies that satisfy the condition $\varepsilon_{LE} \ll 1$. However, when instability wave amplitudes at the lower-branch neutral

stability point are considered, the additional decay that occurs up to this point must be accounted for. This effect complicates the comparison of different measures of receptivity for the case of a parabolic leading edge because the body nose radius and aerodynamic loading exert strong influences on the stability characteristics of the boundary layer.

2.4. Localized Receptivity Theory (Roughness)

Localized receptivity is caused by the interaction of disturbances with short-scale variations in surface geometry. These localized mechanisms can be important even when the variations are small. For example, the localized receptivity of the curvature discontinuity at the ellipse/flat-plate junction could double the overall receptivity (Lin et al. 1992).

Goldstein (1985) developed an asymptotic analysis for localized receptivity, utilizing the triple-deck structure. The viscous flow in the lower deck adjacent to the wall is governed by the LUBLE, showing that short-scale nonparallel mean-flow effects are again responsible for the transfer of energy from the wavelength of the freestream disturbance to that of the instability wave. Kerschen et al. (1990) examined receptivity due to two-dimensional suction strips, Choudhari & Kerschen (1990) extended the theory to three-dimensional wall inhomogeneities, and Kerschen (1991) analyzed the interaction of vortical freestream disturbances with wall inhomogeneities.

Localized receptivity analyses, in which the triple-deck equations are replaced by the exact equations for a small perturbation to a parallel shear flow, have been developed by Choudhari & Streett (1992) and Crouch (1992a). This “finite-Reynolds-number approach” contains exactly the same physical mechanism as the Goldstein (1985) theory. The receptivity arises owing to nonparallel mean-flow effects, which are expressed in terms of a perturbation series with respect to the amplitude of the wall inhomogeneity, identical in form to the localized receptivity analyses of Goldstein, Kerschen, and Choudhari. Crouch (1992b) and Choudhari (1993) have also used the finite-Reynolds-number approach to analyze “distributed receptivity” for wall waviness of wavenumber $\alpha_w \approx \alpha_{TS}$.

Because the finite-Reynolds-number approach is based on the exact equations for small perturbations to a parallel shear flow, it has much in common with Gaster’s (1965) early “OSE-based” analysis of forced receptivity. The approach is ad hoc because the Reynolds number is assumed to be large in certain places and $O(1)$ in others. Also, the OSE approach is only applicable for roughness elements of height $h/L \ll R_L^{-5/8}$, whereas the triple-deck analysis remains valid when $H/L = O(R_L^{-5/8})$. In the small height limit, the triple-deck equations can be solved analytically, whereas the OSE approach requires a numerical solution. However, the OSE approach has certain advantages. The inherent frequency limitation of the triple-deck scaling is no longer present, and the result appears to have higher accuracy with respect to Reynolds number than the leading term of the asymptotic theory. Thus, this approach is useful as a complement to the triple-deck analyses.

3. COMPUTATIONS

Transition is a spatially evolving process, and the spatial direct numerical simulation (DNS) approach is widely applicable because it avoids many of the restrictions that must usually be imposed in other models and is the closest to emulating experiments. For example, no restrictions with respect to the form or amplitude of the disturbances have to be imposed, because no linearizations or special assumptions concerning the disturbances have to be made. Furthermore, this approach allows the realistic treatment of space-amplifying and -evolving disturbances as observed in laboratory experiments. Reed (1994) commented on the various numerical methods, formulations, initial conditions, disturbance inputs, freestream and far-field conditions, and downstream boundary conditions used in spatial simulations. Reed et al. (1998) covered validation issues.

3.1. Leading-Edge Effects

With the spatial computational method, finite curvature can be included in the leading-edge region; this feature was left out of some early unsuccessful receptivity models. Lin et al. (1992) demonstrated this by varying the aspect ratio of the elliptic nose on a flat plate from 3 (blunt) to 9 to 40 (very thin) and showing that the vorticity tends to become singular. By stipulating the plate to have finite curvature at the leading edge, the singularity there is removed and a new length scale is introduced.

Experimentally, the most popular model geometry for receptivity has been the flat plate with an elliptic leading edge. Thus it is reasonable that computational models consider the same geometry. However, the curvature at the juncture between the ellipse and the flat plate is discontinuous and provides a source of receptivity (Goldstein 1985, Goldstein & Hultgren 1987). Lin et al. (1992) confirmed this computationally and then introduced a new leading-edge geometry based on a modified super-ellipse (MSE) given by

$$[(a-x)/a]^{m(x)} + [y/b]^n = 1, \quad 0 < x < a \quad (5a)$$

$$m(x) = 2 + [x/a]^2 \quad \text{and} \quad n = 2, \quad (5b)$$

where $AR = a/b$, b is the half-thickness of the plate and AR is the aspect ratio of the “elliptic” nose. For a usual super-ellipse, both m and n are constants. These super-ellipses have the advantage of continuous curvature (zero) at the juncture with the flat plate as long as $m > 2$ at $x/b = AR$. The MSE, with $m(x)$ given above, has the further advantage of having a nose radius and geometry (hence a pressure distribution) close to that of an ordinary ellipse.

RECEPTIVITY TO FREESTREAM SOUND Saric et al. (1994, 1999) provide an extensive review of the earlier computational efforts, which is not repeated here.

Receptivity results can be expressed either in terms of (a) a leading-edge receptivity coefficient defined as the ratio of the T-S amplitude in the leading-edge

region at $x = O(U_\infty/2\pi f)$ to the freestream-sound amplitude:

$$K_{LE} = |u'_{TS}|_{LE}/|u'_{ac}|_{fs}, \quad (6)$$

or (b) a Branch I receptivity coefficient defined as the T-S amplitude at Branch I normalized with the freestream-sound amplitude:

$$K_I = |u'_{TS}|_I/|u'_{ac}|_{LE}, \quad (7)$$

where $||$ denotes absolute value or rms.

Haddad & Corke (1998) argue that the appropriate receptivity coefficient is K_{LE} because it is based strictly on local properties of the leading-edge region, whereas K_I depends on the pressure gradient history from the leading edge to Branch I. Moreover, because of pressure gradients, K_{LE} decreases with nose radius and K_I increases with nose radius, which could lead to some confusion.

These arguments are compelling, but utilitarian issues sometimes argue for the use of Equation 7. For example, (a) it is impossible for an experiment to measure $|u'_{TS}|_{LE}$, (b) most transition correlation schemes begin with Branch I calculations, and (c) the pressure gradient history can easily be accounted for by OSE calculations up to a region near the leading edge.

Fuciarelli et al. (2000) and Wanderly & Corke (2001) obtain Branch I receptivity coefficients for a 20:1 MSE over a range of frequencies that can be compared with the experiments of Saric & White (1998). The results are shown in Table 1. There is no significant variation with frequency. The agreement between the computations and the experiment is excellent, and we conclude that each validates the other.

Wanderly & Corke (2001) extended the computations over the frequency spectrum at the same Reynolds number for the case of different leading edge shapes. These results are shown in Figure 2. This is an extraordinarily useful result. Not only does one have the Branch I initial amplitude for an amplification factor calculation (given a freestream measurement) but also a very good example of how a leading-edge design needs to proceed.

The DNS results are compared with the theoretical predictions of Goldstein (1983), Kerschen et al. (1990), and Hammerton & Kerschen (1996) where the leading-edge receptivity coefficient is found to be approximately 0.95 (Equation 3). The results of Haddad & Corke (1998) show that the leading-edge receptivity coefficient has a value of approximately 0.47 for a Strouhal number, $S = r_n 2\pi f / U_\infty$,

TABLE 1 Branch I receptivity coefficients for multiple frequencies as predicted by direct numerical simulation (DNS) and compared with the experiments

	Wanderley & Corke (2001)	Fuciarelli et al. (2000)	Saric & White (1998)
Case	DNS	DNS	Experiment
F	90	82–86	88–92
K_I	0.046	0.048	0.050 ± 0.005

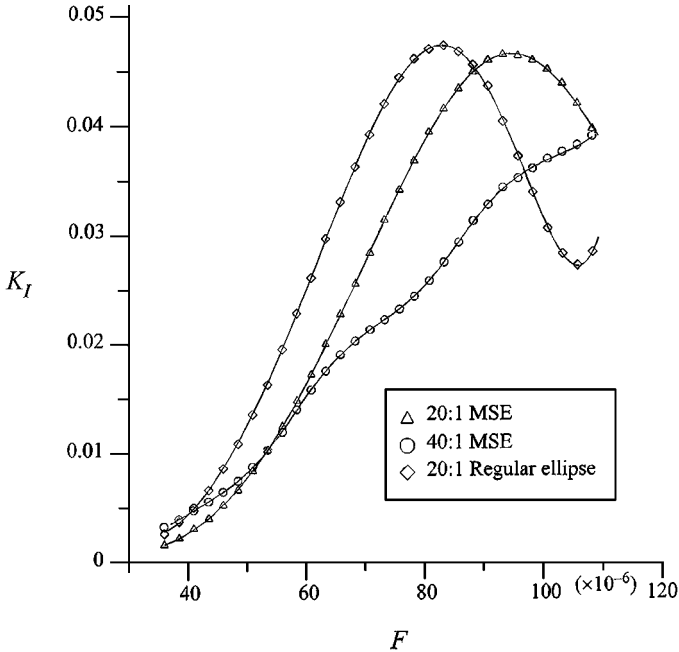


Figure 2 Receptivity coefficients at Branch I as a function of frequency over flat plates with elliptic leading edges; $R_b = 2400$. From Wanderly & Corke (2001).

of 0.01. Using the same Strouhal number, Fuciereilli et al. (2000) marched upstream to an x location of half of the wavelength of the associated instability wave [which approximates the LUBLE region defined by $x2\pi f/U_\infty = O(1)$] and predicted a leading-edge value of approximately 0.75. In an improved calculation, Erturk & Corke (2001) predicted $K_{LE} = 0.64$ at $S = 0.01$ and $K_{LE} = 0.76$ at $S = 0$. All of the computations show a strong decrease in K_{LE} with an increase in S in agreement with theory. In trying to do these comparisons, certain difficulties arise and hence the differences between the calculations are purely technical. The major uncertainty that exists in the DNS (and experiments) is the use of K_{LE} and the choice of streamwise location in the leading-edge region at which the amplitude should be sampled for comparison with the asymptotic theory. However crude these comparisons may be, it is clear that the essential ideas of the asymptotic theory have been validated experimentally and computationally.

FREESTREAM SOUND AT ANGLE OF INCIDENCE With the goal of comparing the results to those of Hammerton & Kerschen (1996, 1997, 2000), Haddad & Corke (1998), Fuciereilli et al. (2000), and Erturk & Corke (2001) numerically studied acoustic waves impinging on the leading edge at angles of incidence α_{ac} . The

TABLE 2 Leading-edge receptivity coefficients for various incidence angles as predicted by DNS and compared with the finite-nose-radius theory

	Fuciarelli et al. (2000)	Hammerton & Kerschen (1996)
α_{ac} (degrees)	K_{LE} DNS	K_{LE} Theory
0	0.75	1.0
5	1.3	1.8
10	2.1	2.6
15	3.2	3.4

comparisons among the three are difficult for a number of reasons. The computations have a semi-infinite body, and the theory has a finite chord. Haddad & Corke (1998) varied both body and incident sound angle of attack, whereas Fuciarelli et al. (2000) fixed the body and varied the incident sound angle. Nevertheless, some highlights are relevant.

Fuciarelli et al. (2000) used an Ansatz (see paper for details) for finite chord and developed a comparison of K_{LE} at $S = 0.01$ (see Table 2). The agreement is excellent and clearly demonstrates the importance of including the effects of the finite nose radius in any receptivity study.

Erturk & Corke (2001) carried out the calculations for the semi-infinite body at different Strouhal numbers (Figure 3). They demonstrated the same qualitative behavior as predicted by theory. Figure 3 is particularly useful for interpreting experimental results in which the sound incidence angle can vary.

RECEPTIVITY TO FREESTREAM VORTICITY The characteristic length scale for free-stream spanwise vorticity is the convective wavelength $U_\infty/2\pi f$, which is approximately three times that of the amplified T-S wave at that frequency.

Buter & Reed (1994) simulated the receptivity of the laminar boundary layer on a flat plate by using the same techniques and geometries as Lin et al. (1992). A simple model of time-periodic freestream spanwise vorticity was introduced at the upstream computational boundary. This signal was decomposed into a symmetric and asymmetric streamwise velocity component with respect to the stagnation streamline. The effect of a transverse-velocity component at the leading edge could be ascertained, as the asymmetric-velocity case had this feature, whereas the symmetric-velocity did not. Buter & Reed (1994) found the following:

- (a) As the disturbance convected past the body, it was ingested into the upper part of the boundary layer, decaying exponentially toward the wall. This is consistent with the findings of Kerschen (1989) and Parekh et al. (1991).
- (b) Different wavelengths were evident in the boundary-layer response. Signals at the T-S wavelength were dominant near the wall, whereas toward the edge of the boundary layer, disturbances of the freestream convective wavelength

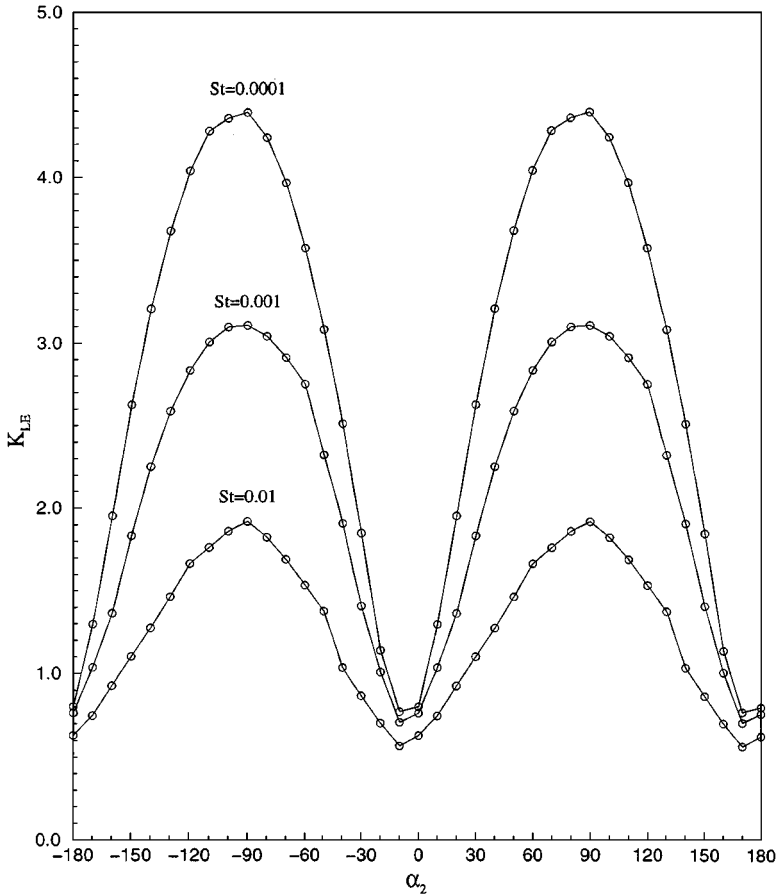


Figure 3 Variation of the leading-edge receptivity coefficient with respect to the acoustic wave angle as a function of Strouhal number. From Erturk & Corke (2001).

were observed. This is consistent with the experimental observations of Kendall (1991).

- (c) For the particular geometric and flow conditions considered in this study, receptivity to vorticity was smaller than receptivity to sound by a factor of approximately three.
- (d) The T-S responses to the symmetric and asymmetric freestream velocity perturbations were linear up to freestream amplitudes of 4.2% U_∞ and 2.1% U_∞ , respectively. For plane freestream sound, Lin et al. (1992) had found the receptivity to be linear up to a freestream amplitude of about 5% U_∞ .

3.2. Observation

For each configuration under consideration, the complete integrated picture of geometry and associated pressure gradients (both favorable and adverse) must be included in any meaningful evaluation of receptivity, and it is here that computations by spatial DNS can excel. A variety of different freestream disturbances can be implemented with this technique and the response of the boundary layer quantified and catalogued.

Spatial simulations are still too expensive to use for routine design, and at present, we cannot provide a completely resolved solution all the way through transition to turbulence even on a flat plate. However, an important and exciting role for the simulation is in the development and calibration of simpler models. The abundance of information provided is invaluable and complements any experimental effort.

Moreover, these results provide the link between the freestream and the initial boundary-layer response and can provide the upstream conditions for further DNS or parabolized stability equation (PSE) (Herbert 1997) simulations marching through the transition process toward turbulence. Bertolotti (1997) provides an example of a PSE application, which is discussed in Section 4.3.1.

4. EXPERIMENTS

The typical model for boundary-layer experiments is the zero-pressure-gradient flat plate. In most cases, the flat plate is preceded by an elliptical leading-edge attachment. Here, the coupling between the long-wavelength acoustic disturbance and a T-S wave occurs in four regions: the leading edge, the discontinuity in surface curvature at the flat-plate/leading-edge junction, the presence of localized pressure gradients, and any surface inhomogeneities such as roughness, suction slots, or filler material used for the flat-plate/leading-edge gap. A complete critical review of earlier receptivity studies is reported by Nishioka & Morkovin (1986), who concluded that all experiments prior to 1986 were flawed to some extent.

Nishioka & Morkovin (1986) specifically mentioned that previous experiments had been inconclusive because of (a) poor quantitative characterization of the forcing field along the outer edge of the boundary layer, (b) inadequate local information on the fluctuations in the boundary layer in the region where the stimulated unstable response starts growing, (c) lack of documentation of potentially singular diffraction fields around the leading edge and/or the singular effects of vibrations of the leading edge, and (d) excessive forcing disturbance levels. Care with (a) and (b) allows different receptivity mechanisms to be sorted out and attention to (c) and (d) isolates other receptivity paths and nonlinearities. Added to these requirements is the general experimental caveat: First do the linear problem correctly and then provide initial conditions for the theory and computations.

4.1. Measurement Techniques

Prior to Kendall (1990), Wlezien (1989), and Wlezien et al. (1990), acoustic receptivity measurements suffered from contamination of the T-S signal by background disturbances. When an external sound field is used as a source of disturbance energy, the boundary-layer measurement at a particular frequency will contain probe vibrations and a sound-wave component (Stokes layer) in addition to the T-S wave. If these signals are of comparable amplitude, one can not extract the T-S amplitude without some special separation technique. It is for this reason that older publications do not show typical T-S profiles. Thus, the first step in any receptivity experiment is to isolate the T-S wave from the other fluctuations at the same frequency. A review of the different methods follows.

LARGE AMPLITUDE T-S WAVE The simplest solution is to take advantage of the exponential growth of the T-S wave and measure far enough downstream from the receptivity source. The T-S wave amplitude is then significantly higher than the background disturbances and can be measured directly. This technique was used by Saric et al. (1991) in two-dimensional roughness receptivity experiments. Different techniques are needed if one must measure close to the receptivity source or if the receptivity source is weak.

REMOVABLE RECEPTIVITY SOURCE Spencer et al. (1991) studied the receptivity of three-dimensional roughness elements by measuring the near-field disturbance patterns. The receptivity source was weak and the Stokes wave and the T-S wave were of comparable amplitude. In this case, the roughness element was removable, and the amplitude and phase of the hotwire signal were measured with and without the roughness. The two signals were then subtracted in the complex plane. Therefore, without specifically determining the components of the background signal (which may include other receptivity sources), it is possible to isolate directly the T-S wave.

KENDALL GAUGE Kendall (1990) provided an effective technique for separating the T-S wave from the background disturbances. Here, one senses wall pressure fluctuations at two pressure ports spaced at approximately half the T-S wavelength. The differential pressure is then twice that of the T-S wave, whereas the long-wavelength pressure fluctuations due to freestream turbulence are cancelled with typically a 100:1 rejection ratio. With a distribution of pressure-port pairs, one obtains immediately the spatial behavior of the T-S wave. This method is recommended in cases of freestream turbulence. However, it does not work with acoustic waves because the pressure disturbance is proportional to the sound speed, whereas the T-S wave pressure disturbance is proportional to the freestream speed. Thus, the 100:1 rejection of the gauge is swamped by the 100:1 ratio in pressure disturbances.

COMPLEX PLANE RESOLUTION Wlezien (1989) and Wlezien et al. (1990) studied the receptivity of suction slots and leading edges. Taking advantage of the fact that the acoustic wavelength is two orders of magnitude larger than the T-S wavelength, Wlezien used polar plots to separate the long-wavelength Stokes wave from the short-wavelength T-S wave. Disturbance amplitudes and phases were measured at a series of points constant in y and z but closely spaced over a T-S wavelength in x . In this short distance, the phase of the long-wavelength acoustic signal varies only slightly, whereas the phase of the T-S wave varies over 2π . When plotted in the complex plane, the total signal forms a spiral. The background signal, consisting of acoustic and vibrational fluctuations, is the vector from the origin to the center of the spiral, and the T-S wave is the vector from the center to the total signal. Subtraction in the complex plane produces the T-S wave amplitude and phase. Examples of such a measurement can be found in Wlezien (1994) and Saric et al. (1994, 1995).

INDEPENDENT RESOLUTION OF THE STOKES WAVE One might try to measure the Stokes wave at a mean velocity low enough so no T-S wave is present, yet high enough to keep calibration of the hotwire, but this technique has not been successful. The acoustic field of a closed-circuit wind tunnel is quite complicated and appears to be affected by wind-tunnel speed.

RESOLUTION OF DUCT ACOUSTICS The downstream traveling wave reflects in the diffuser and returns an upstream traveling wave giving a standing wave pattern in the test section. This is not a problem for localized receptivity sites because one need only measure the freestream amplitude at the local position. For distributed receptivity sites, Wiegel & Wlezien (1993) used a second acoustic wave from the diffuser, cancelled the standing wave pattern, and created a streamwise-uniform sound amplitude distribution. This technique is now considered the standard means for obtaining uniform sound fields.

The use of a steady acoustic signal can force the wake and create upstream influence when the model splits the test section. The data of Saric et al. (1995) show a very narrow passband of amplified frequencies. This behavior was not predicted and was at odds with OSE results. Additional measurements of this flow field concentrated on the difference of the fluctuations on both sides of the plate and showed that the continuous sound signal was forcing a resonance in the wake causing an asymmetric oscillation that fed back to the leading edge in the form of fluctuations transverse to the leading edge. Thus these experiments were biased.

PULSED-SOUND TECHNIQUE Saric et al. (1995) suggested a new technique to measure the T-S wave amplitude without upstream forcing of the wake oscillations. The technique uses pulsed sound and is simple, effective, and lends itself to understanding the behavior of the T-S wave. From linear theory, the maximum of the T-S wave propagates at approximately one third of the freestream speed (about 1% of the speed of the downstream-traveling sound wave). Using this fact, the

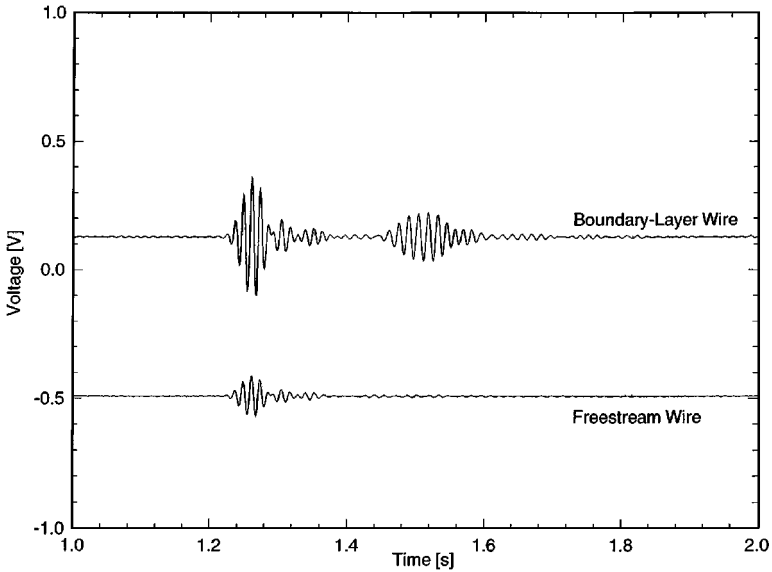


Figure 4 Time traces of freestream wave and boundary-layer wave. From Saric et al. (1999).

traveling T-S wave can be isolated from the acoustic disturbance and associated Stokes wave by sending bursts of sound into the test section. The initial sound burst is measured first, and fractions of a second later, after the sound wave has passed, the slower-traveling T-S wave is measured.

Figure 4 shows a time trace depicting the sound-burst wave sensed by hotwires in the freestream and boundary layer and the trailing T-S wave measured by the boundary-layer wire for $R = 1140$, $F = 56$, $f = 80$ Hz and $x = 1.8$ m. The T-S wave profile obtained with this method compares very well with OSE solutions. The agreement between theory and experiment indicates this is a versatile technique with a wide range of application. Kanner & Schetz (1999) recently used this technique in a study of sound-induced transition on an airfoil.

There are three ways to implement this technique: (a) Use the rms amplitude of the wave packet, as suggested by Saric et al. (1995); (b) use the magnitude of the complex Fourier coefficient for each frequency present in the wave packet (Saric & White 1998); and (c) analyze the signal in the frequency domain (White et al. 2000).

The frequency-domain approach of White et al. (2000) appears to be the best means to correctly describe the receptivity and linear amplification process of multiple-frequency signals. This is because as wave packets travel downstream, high-frequency components of the spectra, which are present initially owing to the finite extent of the pulse, decay. Meanwhile, the low-frequency components in the amplified T-S band grow.

A feature of short sound bursts is that because they are limited in the time domain, they are extended in the frequency domain. Thus, a single sound pulse (a single frequency sine wave within an amplitude envelope) covers a wide frequency range. In many cases the pulse spectrum covers the entire T-S wavelength band. Therefore, using a pulsed-sound approach eliminates the distinction between single frequency and broadband input.

4.2. Leading-Edge Receptivity to Freestream Sound

Saric & White (1998) conducted a series of leading-edge receptivity experiments on a 20:1 modified super ellipse given in Equation 5 where $a = 4.76$ mm and $b = 190.5$ mm. The leading edge is machined directly on a 4000 mm (chord) \times 1370 mm (span) \times 9.53 mm (thickness) flat-plate. This design moves the pressure minimum toward the leading edge, eliminates the curvature discontinuity at the juncture, and eliminates any discontinuities associated with the ellipse/flat-plate juncture that could serve as a receptivity mechanism. Simultaneous static pressure measurements on each side of the leading edge are used to adjust the flap for symmetric flow. For the linear experiments, the sound pressure level in the test section is limited to 95 dB ($p' = \rho c_a u'_{\text{rms}}; 20 \mu$ Pa reference) to avoid excessive forcing. This gives a $|u'_{ac}|_{fs} = O(10^{-4} U_\infty)$.

The T-S waves are measured as far downstream as possible, typically just before the Branch II neutral point, (a) to obtain the strongest possible disturbance signal and (b) to generate the greatest separation possible between the Stokes and T-S wave packets. In generating the receptivity coefficients, linear theory is used to relate the T-S amplitudes measured downstream to the amplitudes at the Branch I neutral point. The receptivity process is shown to be linear over several orders of magnitude of forcing amplitude.

The pulsed-sound technique has been used to measure T-S mode shapes. The observed mode shapes match linear theory predictions and demonstrate convincingly that the pulsed-sound/Fourier technique of White et al. (2000) is a valid means of measuring relative disturbance amplitude. The results are compared with DNS in Table 1.

4.3. Receptivity to Freestream Turbulence or Vorticity

Receptivity to freestream turbulence is a crucial problem that has resisted a straightforward solution on the experimental side. Recall that the objective of receptivity is to provide a coupling coefficient between a freestream disturbance measurement and the boundary-layer response. This objective has to be kept in mind when interpreting the results of published work. We know that an increase in freestream turbulence increases the amplitude of T-S waves and lowers the transition Reynolds number. One should hope that the mechanism is linear for at least part of the range. However, this is not the case and this is only one of the difficulties.

The effects of vorticity and/or freestream turbulence on a laminar boundary layer have been studied by Klebanoff (1971), Arnal & Juillen (1978), Kachanov

et al. (1978), Kosorygin et al. (1988), Suder et al. (1988), Gulyaev et al. (1989), and Kendall (1984, 1985, 1990, 1991, 1998). Nishioka & Morkovin (1986) and Reshotko (1994) review the early literature. With the advent of work on transient growth and bypass transition, a series of experimental papers from KTH in Sweden (Westin et al. 1994, Boiko et al. 1994, Westin et al. 1998, Bakchinov et al. 1998, Alfredsson & Matsubara 2000, Matsubara & Alfredsson 2001) and others (Grek et al. 1990, 2000; Jonáš et al. 2000; Ustinov et al. 2000) have demonstrated that the problem of receptivity to freestream turbulence is directly coupled to transient growth of nonorthogonal modes.

THE KENDALL EXPERIMENT Over the past 20 years, Kendall (1998) has developed a careful and thoroughly considered experimental setup in which the freestream turbulence can systematically be controlled and the initiation of T-S waves in the boundary layer can be examined. The specific goal of these experiments was to relate the T-S wave amplitude to the measured freestream turbulence amplitude.

In contrast to acoustic forcing, freestream turbulence initiates three distinct motions within the boundary layer. The first motion is a sustained, streaky ($z \approx 2\delta$), high amplitude ($|u'| \approx 5 - 10\% U_\infty$) motion, which is probably due to stretching of the ingested freestream vorticity and the growth of transient modes. This is historically called the Klebanoff mode. The second is an outer-layer oscillation at T-S frequencies that grows weakly in the stream direction. These modes may have some connection with the continuous spectrum of the OSE, but this is not clear. The third is the usual T-S mode, which exhibits higher growth rates. Kendall found the following:

- (a) The T-S waves are wave-packet-like and are of lower amplitude than the other two modes. Although some qualitative characteristics of the observed wave packets resemble those of the Gaster & Grant (1975) experiments, the growth rates and spreading angles are much different. Thus, an internally generated wave packet behaves differently than an externally generated wave packet.
- (b) The Klebanoff modes were unchanged by leading-edge bluntness and lift, and therefore Kendall (1991) concluded that these modes play no part in the T-S wave development. These modes grow as $x^{1/2}$, and Luchini (2000), who predicted the same behavior, demonstrated their connection to transient growth.
- (c) Detailed measurements show that, whereas the freestream is a stationary broadband forcing, the boundary-layer response is in the form of wave packets that occur sporadically and that have random amplitudes from one instance to another. These generally grow in strength and number of oscillation cycles during their downstream passage. The signal appears to be rather quiescent in the intervals between the occurrence of packets or bursts. One concludes, therefore, that an apparently stationary random input from the freestream produces a stochastic response within the boundary layer.

Kendall has tried, without success, different correlation schemes to identify a feature in the freestream that causes the sporadic behavior of the packets. Something must be present in the freestream that cannot be measured.

- (d) Kendall (1991) showed how the average amplitude varies as a function of turbulence level at different streamwise positions for one particular frequency. The behavior is nonlinear over almost the entire range of Reynolds numbers. Kendall (1991) also described an amplitude dependence for the growth rates of the wave packets. The growth depends not only on the freestream turbulence level but also on the amplitude of the packet under conditions of fixed freestream turbulence. There are any number of conjectures as to the source of the nonlinearity. A first guess is to postulate that the turbulence is continuously feeding into the generation of the T-S wave along the stream direction. This supposes another, as yet unknown, receptivity mechanism in addition to the leading edge.

Space constraints do not permit the complete treatment that this challenging work deserves. There are valuable data in the papers but obviously no direct conclusion regarding receptivity. Because of the strong three-dimensional nature of the initial disturbances and the subsequent nonlinear development of the resulting T-S waves, the measurements are extraordinarily difficult.

Recently, Bertolotti (1997) and Su & Herbert (2000) approached the Kendall data as a forced receptivity problem using PSE. They were able to model much of the observed behavior. It appears as though the elusive coupling coefficient between the freestream and the boundary layer is still missing. The value of the PSE in this case is to provide the details that an OSE solution cannot provide and to carry the computations to transition.

THE KTH EXPERIMENTS The goal of the KTH experiments was the determination of the role of transient growth. This carefully sequenced set of experiments (Westin et al. 1994, 1998; Boiko et al. 1994; Bakchinov et al. 1998; Alfredsson & Matsubara 2000; Matsubara & Alfredsson 2001) successfully showed the connection between the streaky structure and transient growth. These series of experiments covered a great deal of new material from the early development of instabilities to secondary instabilities and breakdown. The results of this work as it applies to receptivity are as follows:

- (a) The boundary layer responds nonlinearly to an increase in freestream turbulence as first shown by Kendall (1991). Again, there is the conjecture that there is a continuous receptivity process along the streamwise extent of the boundary layer.
- (b) Transient (algebraic) growth plays a more important role in the boundary-layer response as the freestream turbulence is increased. Referring back to Figure 1, the path to transition for the lowest freestream disturbance levels (A) does not include transient growth. As the freestream amplitude

is increased, a point is reached where the primary OSE modes are bypassed completely.

- (c) Transient growth plays a particularly strong role in the presence of distributed surface roughness.
- (d) As with the Kendall experiments, a coupling coefficient has not been determined.

ISOLATED VORTICAL DISTURBANCES Kachanov et al. (1978) placed a vibrating ribbon upstream of a 60:1 ellipse/flat plate and entrained weak disturbances into the boundary layer when the ribbon wake was more or less aligned with the stagnation line. When the ribbon was displaced off the line of symmetry, no boundary-layer response was observed. Buter & Reed (1993) presented results of a DNS study on essentially the same problem as Kachanov et al. (1978). They introduced both symmetric and asymmetric transverse vorticity upstream of an elliptical leading edge and demonstrated that T-S waves are generated within the boundary layer. However, no T-S waves are generated if the vorticity is displaced off the centerline. Kerschen (1991) also showed that the leading edge, a wall hump, or surface inhomogeneity is needed for the generation of T-S waves.

In related work, Parekh et al. (1991) attempted to create T-S waves through the interaction of transverse vortical freestream disturbances with the leading edge. They used an oscillating array of 10 ribbons upstream of the leading edge to generate a periodically varying vortical flow. In spite of using all of the caution and care required of such an experiment, they were unable to measure T-S waves from either the leading edge or the step. The work of Kerschen (1991) and Buter & Reed (1993) indicate that a vortical flow should indeed create T-S waves. Because the experiments by Kachanov et al. (1978) are not as well documented as those by Parekh et al. (1991), it is difficult to sort out the differences between the two.

Dietz (1999) introduced vortical disturbances in the freestream with the wake of a vibrating ribbon. He concentrated on the interaction of this disturbance with a two-dimensional roughness element on the flat plate. His receptivity function is somewhat higher than the Kerschen asymptotic theory or the Choudhari computations but the trends are correct. This is really the first clean experiment in which a two-dimensional T-S wave was created with a vortical freestream disturbance.

4.4. Receptivity of Roughness to Freestream Sound

Wlezien (1989) and Wlezien et al. (1990) addressed the acoustic receptivity of porous suction slots. These sets of experiments were the first to use the modern techniques discussed in Section 4.1 to measure T-S waves in an acoustic-receptivity process. Kerschen et al. (1990) analyzed localized receptivity due to porous suction strips and showed that two receptivity mechanisms are present. One is due to the mean-flow adjustment and is similar to receptivity caused by wall roughness elements, whereas the other is caused by scattering due to the finite acoustic admittance.

With their 6:1 aspect-ratio leading edge, amplitude versus x curves are presented for three different frequencies for a solid surface, a 0.1 mm open slot, and a 7 mm porous strip. Although the width is not optimal according to theory (Kerschen 1989), the data clearly show the enhancement of the T-S amplitude in the case of porous strips. However, because there was also significant receptivity from the leading edge and only the frequency was varied, it is not possible to define a receptivity coefficient in the usual sense, and thus these data can only be interpreted qualitatively.

Saric et al. (1991) studied the receptivity of two-dimensional roughness to sound with minimal leading-edge effects. They used two-dimensional roughness strips that were 40- μm thick and 25-mm wide. The width corresponded to the half wavelength of the T-S wave ($\lambda_{TS} = 50$ mm) at $F = 50$. They correlated the effect of the thickness of the roughness element with a roughness Reynolds number R_k . Here, R_k is based on the local velocity at $y = k$ and the roughness height k , $R_k = U(k)k/\nu$.

In a comparison with the theory, the effect of roughness height on the receptivity process was determined by varying the thickness of the roughness element over a range of 45–270 μm . They showed that the T-S response varies almost linearly with roughness height, over the range of 40–120 μm ($R_k = 0.5$ –5.0). The curves of T-S amplitude versus roughness height at two sound-pressure levels show almost the same slope up to a certain point near 200 μm . The slopes change as a function of both k and sound level. The receptivity mechanism is now nonlinear.

The linear behavior is predicted quite accurately by Crouch (1991, 1992a), who used a local receptivity analysis on the experimental data. His calculations cut right through the data. The linear results were also predicted by Choudhari & Streett (1992) and Nayfeh & Ashour (1994); Nayfeh & Ashour were also able to account for the leading edge receptivity. The departure from linear behavior occurs in the range of $k = 180$ –225 μm . Bodonyi et al. (1989) and Bodonyi (1990) used a nonlinear triple-deck analysis and computation, which showed that the departure from linearity occurs when the roughness height exceeds that of the lower viscous deck, i.e., when $k \geq \varepsilon^5 L$, where $\varepsilon = R_x^{-1/8}$ and $L = x$. For the conditions of this experiment, $R_x = (590)^2$, $x = 460$ mm, and $\varepsilon^5 L = 158$ μm . Thus, this agreement provides a firm explanation for the range of linearity of these experiments. This was put on firmer ground by Crouch & Spalart (1995), who ran a DNS in the nonlinear range for two-dimensional suction strips as the receptivity elements. They showed the same trends in the nonlinear behavior. Recently, Airiau et al. (2000) used the adjoint PSE method to compare with the above experiments and to those by Crouch (1992a). The agreement in the linear range was quite good. Therefore, the theory and calculations seem to indicate that the two-dimensional roughness problem is very well understood.

Kosorygin et al. (1995) reported on experiments where the position of the roughness element is changed with respect to the leading edge in a manner similar to the work by Kosorygin & Polyakov (1990). Here, the T-S wave generated by the roughness element interfered constructively or destructively with the T-S wave generated

by the leading edge. They showed that there exists a particular x position where the destructive interference is a maximum and the T-S wave amplitude is below the leading-edge (no roughness) value. Kosorygin (2000) has extended this work to include the role of both adverse and favorable streamwise pressure gradients.

With the idea of verifying the linear theory of Choudhari & Kerschen (1990) and the nonlinear work of Tadjfar & Bodonyi (1992), Spencer et al. (1991) worked on experiments with three-dimensional roughness elements. Because of the difficulty of measuring close to the roughness element, the near-field results are not reliable, and only moderate agreement with the theory was reached in the far field. This work has recently been taken up by Cullen & Horton (2000), who experimentally verified the qualitative aspects of the theory.

Wiegel & Wlezien (1993) considered distributed two-dimensional roughness as receptivity in an effort to provide a data base for the theoretical work of Choudhari (1993) and Crouch (1992b). When multiple receptivity elements are used, it is important to have a uniform sound field across the elements so that the same normalizing $|u'_{ac}|_{fs}$ can be used in the receptivity coefficient. Using the techniques presented in Resolution of Duct Acoustics (above), the agreement between theory and experiment is very good for all aspects of the problem. The details are also reviewed in Wlezien (1994). Thus, the receptivity of distributed two-dimensional roughness is on firm theoretical ground.

In a series of careful experiments, King & Breuer (2001) extended the work of Wiegel & Wlezien (1993) by considering oblique (or swept) distributed roughness strips. They expanded the data set for two-dimensional roughness and successfully compared with the results of Crouch (1992b). The receptivity for oblique roughness is approximately the same as that of two-dimensional roughness; however, the three-dimensional waves that are generated exhibit very different stability behavior.

CONCLUSIONS

The past decade has seen considerable progress in the understanding of receptivity mechanisms. The agreement between theory and experiment on two-dimensional roughness is remarkable. Experimental issues on leading-edge receptivity have been settled, and DNS has been established as a viable framework for more detailed studies on different geometries. Challenges still exist in the areas of freestream turbulence and bypasses. We expect progress to occur when theoretical, computational, and experimental methods are combined to address these important problems.

ACKNOWLEDGMENTS

This work was sponsored (in part) by the Air Force Office of Scientific Research, USAF, under grant numbers NA-90-065 (E.J.K.), F49620-00-0075 (W.S.S. and H.L.R.); NASA Langley Research Center grants NASA-1-1135 (E.J.K.) and

NAG-1-1158 (H.L.R.); and the NSF Awards for Women in Science and Engineering EID-90-22523 (H.L.R.). The authors also thank Professor Thomas Corke for valuable discussions and his permission to use some of his figures.

Visit the Annual Reviews home page at www.AnnualReviews.org

LITERATURE CITED

- Airiau C, Walther S, Bottaro A. 2000. Non-parallel receptivity and the adjoint PSE. See Fasel & Saric 2000, pp. 57–64
- Alfredsson PH, Matsubara M. 2000. Free-stream turbulence, streaky structures and transition in boundary-layer flows. *AIAA Pap.* 2000–2534
- Andersson P, Berggren M, Henningson DS. 1999. Optimal disturbance and bypass transition in boundary layers. *Phys. Fluids* 11:134–50
- Arnal D. 1994. Predictions based on linear theory. See Saric 1994a, pp. 3.1–16
- Arnal D, Juillen JC. 1978. Contribution experimentale a l'etude de la receptivite d'un couche limite laminaire, a la turbulence de l'ecoulement general. *ONERA Rt. Tech. 1/5018 AYD*
- Arnal D, Michel R, eds. 1990. *Laminar-Turbulent Transition, Vol. III*. New York: Springer. 710 pp.
- Bakchinov AA, Westin KJA, Kozlov VV, Alfredsson PH. 1998. Experiments on localized disturbances in a flat plate boundary layer. Part 2: interaction between localized disturbances and TS-waves. *Eur. J. Mech. B Fluids* 17:847–73
- Bayley BJ, Orszag SA, Herbert T. 1988. Instability mechanisms in shear-flow transition. *Annu. Rev. Fluid Mech.* 20:359–91
- Bertolotti FP. 1997. Response of the Blasius boundary layer to free-stream vorticity. *Phys. Fluids* 9:2286–99
- Bodonyi RJ. 1990. Nonlinear triple-deck studies in boundary-layer receptivity. *Appl. Mech. Rev.* 43 (Pt. 2):S158–66
- Bodonyi RJ, Welch WJC, Duck PW, Tadjfar M. 1989. A numerical study of the interaction between unsteady freestream disturbances and localized variations in surface geometry. *J. Fluid Mech.* 209:285–308
- Boiko AV, Westin KJA, Klingmann BGB, Kozlov VV, Alfredsson PH. 1994. Experiments in a boundary layer subjected to freestream turbulence. Part 2: the role of TS-waves in the transition process. *J. Fluid Mech.* 281: 219–45
- Breuer KS, Grimaldi ME, Gunnarsson J, Ullmar M. 1996. Linear and nonlinear evolution of boundary-layer instabilities generated by acoustic receptivity mechanisms. *AIAA Pap.* 96–0183
- Buter TA, Reed HL. 1993. Numerical investigation of receptivity to freestream vorticity. *AIAA Pap.* 93–0073
- Buter TA, Reed HL. 1994. Boundary-layer receptivity to freestream vorticity. *Phys. Fluids* 6:3368–79
- Choudhari M. 1993. Boundary-layer receptivity due to distributed surface imperfections of a deterministic or random nature. *Theor. Comp. Fluid Dyn.* 4:101–17
- Choudhari M, Kerschen EJ. 1990. Instability wave patterns generated by interaction of sound waves with three-dimensional wall suction or roughness. *AIAA Pap.* 90–0119
- Choudhari M, Streett C. 1992. A finite Reynolds number approach for the prediction of boundary-layer receptivity in localized regions. *Phys. Fluids A* 4:2495–514
- Choudhari M, Streett C. 1994. Theoretical predictions of boundary-layer receptivity. *AIAA Pap.* 94–2223
- Corke TC. 1990. Effect of controlled resonant interactions and mode detuning on turbulent transition in boundary layers. See Arnal & Michel 1990, pp. 151–78
- Crouch JD. 1991. Initiation of boundary-layer

- disturbances by nonlinear mode interactions. See Reda et al. 1991, pp. 63–68
- Crouch JD. 1992a. Localized receptivity of boundary layers. *Phys. Fluids A* 4:1408–14
- Crouch JD. 1992b. Non-localized receptivity of boundary layers. *J. Fluid Mech.* 244:567–81
- Crouch JD. 1994. Receptivity of boundary layers. *AIAA Pap.* 94–2224
- Crouch JD, Spalart PR. 1995. A study of non-parallel and nonlinear effects on the localized receptivity of boundary layers. *J. Fluid Mech.* 290:29–37
- Cullen LM, Horton HP. 2000. Acoustic receptivity in boundary layers with surface roughness. See Fasel & Saric 2000, pp. 43–50
- Dietz AJ. 1999. Local boundary-layer receptivity to a convected free-stream disturbance. *J. Fluid Mech.* 378:291–317
- Erturk E, Corke TC. 2001. Boundary-layer leading-edge receptivity to sound at incidence angles. *J. Fluid Mech.* 444:383–407
- Fasel HF, Saric WS, eds. 2000. *Laminar-Turbulent Transition V*. Berlin: Springer. 686 pp.
- Fuciarelli DA, Reed HL, Lyttle I. 2000. Direct numerical simulation of leading-edge receptivity to sound. *AIAA J.* 38:1159–65
- Gaster M, Grant I. 1975. An experimental investigation of the formation and development of a wave packet in a laminar boundary layer. *Proc. R. Soc. Lond. Ser. A* 347:253
- Gaster M. 1965. On the generation of spatially growing waves in a boundary layer. *J. Fluid Mech.* 22:433–41
- Goldstein ME. 1983. The evolution of Tollmien-Schlichting waves near a leading edge. *J. Fluid Mech.* 127:59–81
- Goldstein ME. 1985. Scattering of acoustic waves into Tollmien-Schlichting waves by small streamwise variations in surface geometry. *J. Fluid Mech.* 154:509–29
- Goldstein ME, Hultgren LS. 1987. A note on the generation of Tollmien-Schlichting waves by sudden surface-curvature change. *J. Fluid Mech.* 181:519–25
- Goldstein ME, Hultgren LS. 1989. Boundary-layer receptivity to long-wave disturbances. *Annu. Rev. Fluid Mech.* 21:137–66
- Goldstein ME, Sockol PM, Sanz J. 1983. The evolution of Tollmien-Schlichting waves near a leading edge. Part 2. Numerical determination of amplitudes. *J. Fluid Mech.* 129:443–53
- Grek HR, Kozlov VV, Ramazanov MP. 1990. Receptivity and stability of the boundary layer at a high turbulence level. See Arnal & Michel 1990, pp. 511–21
- Grek HR, Kozlov VV, Sboev DS. 2000. Experiments on the receptivity of a boundary layer to a localized free-stream disturbance. See Fasel & Saric 2000, pp. 131–36
- Grosch CE, Salwen H. 1983. Oscillating stagnation point flow. *Proc. R. Soc. Lond. Ser. A* 384:175–90
- Gulyaev AN, Kozlov VE, Kuznetsov VR, Mineev BI, Sekundov AN. 1989. Interaction of a laminar boundary layer with external turbulence. *Izv. Akad. Nauk SSR, Mekh. Zhid. Gaza* 5:55 (see *Fluid Dyn.* 1990. 24:700).
- Haddad O, Corke TC. 1998. Boundary-layer receptivity to freestream sound on parabolic bodies. *J. Fluid Mech.* 368:1–26
- Hammerton PW, Kerschen EJ. 1992. Effect of nose bluntness on leading-edge receptivity. See Hussaini et al. 1992, pp. 441–51
- Hammerton PW, Kerschen EJ. 1996. Boundary-layer receptivity for a parabolic leading edge. *J. Fluid Mech.* 310:243–67
- Hammerton PW, Kerschen EJ. 1997. Boundary-layer receptivity for a parabolic leading edge. Part 2. The small Strouhal number limit. *J. Fluid Mech.* 353:205–20
- Hammerton PW, Kerschen EJ. 2000. Effect of leading-edge geometry and aerodynamic loading on receptivity to acoustic disturbances. See Fasel & Saric 2000, pp. 37–42
- Heinrich RA, Kerschen EJ. 1989. Leading-edge boundary-layer receptivity to free-stream disturbance structures. *ZAMM* 69: T596
- Henningson DS, Lundbladh A, Johansson AV. 1993. A mechanism for bypass transition from localized disturbances in wall-bounded shear flows. *J. Fluid Mech.* 250:169–207
- Herbert T. 1997. Parabolized stability equations. *Annu. Rev. Fluid Mech.* 29:245–83

- Hultgren LS, Gustavsson LH. 1981. Algebraic growth of disturbances in a laminar boundary layer. *Phys. Fluids* 24:1000–4
- Hussaini MY, Kumar A, Streett CL, eds. 1992. *Instability, Transition, and Turbulence*. Berlin: Springer. 620 pp.
- Jonáš P, Mazur O, Uruba V. 2000. On the receptivity of the by-pass transition to the length scale of the outer stream turbulence. *Eur. J. Mech. B Fluids* 19:707–22
- Kachanov YuS. 2000. Three-dimensional receptivity of boundary layers. *Eur. J. Mech. B. Fluids* 19:723–44
- Kachanov YuS, Kozlov VV, Levchenko VYa. 1978. Origin of Tollmien-Schlichting waves in boundary layers under the influence of external disturbances (in Russian). *Mek. Zhid. i Gaza*, 5:85 (see *Fluid Dyn* 1979 13:704–11)
- Kanner HS, Schetz JA. 1999. The evolution of an acoustic disturbance up to transition in the boundary layer on an airfoil. *AIAA Pap. No. 99–3791*
- Kato T, Fukunishi Y, Kobayashi R. 1997. Artificial control of the three-dimensionalization process of T-S waves in boundary-layer transition. *JSME Intl. J. Ser. B* 40:536–41
- Kendall JM. 1984. Experiments on the generation of Tollmien-Schlichting waves in a flat-plate boundary layer by weak freestream turbulence. *AIAA Pap. 84–0011*
- Kendall JM. 1985. Experimental study of disturbances produced in a pre-transitional laminar boundary layer by weak freestream turbulence. *AIAA Pap. 85–1695*
- Kendall JM. 1990. Boundary-layer receptivity to freestream turbulence. *AIAA Pap. 90–1504*
- Kendall JM. 1991. Studies on laminar boundary-layer receptivity to freestream turbulence near a leading edge. See Reda et al. 1991, pp. 23–30
- Kendall JM. 1998. Experiments on boundary-layer receptivity to freestream turbulence. *AIAA Pap. 98–0530*
- Kerschen EJ. 1989. Boundary-layer receptivity. *AIAA Pap. 89–1109*
- Kerschen EJ. 1991. Linear and nonlinear receptivity to vortical freestream disturbances. See Reda et al. 1991, pp. 43–48
- Kerschen EJ, Choudhari M, Heinrich RA. 1990. Generation of boundary instability waves by acoustic and vortical freestream disturbances. See Arnal & Michel 1990, pp. 477–88
- King RA, Breuer KS. 2001. Acoustic receptivity and evolution of two-dimensional and oblique disturbances in a Blasius boundary layer. *J. Fluid Mech.* 432:69–90
- Klebanoff PS. 1971. Effect of freestream turbulence on the laminar boundary layer. *Bull. Am. Phys. Soc.* 10:1323
- Kobayashi R, ed. 1995. *Laminar-Turbulent Transition IV*. Berlin: Springer. 532 pp.
- Kobayashi R, Fukunishi Y, Nishikawa T, Kato T. 1995. The receptivity of flat-plate boundary layers with two-dimensional roughness elements to freestream sound and its control. See Kobayashi 1995, pp. 507–14
- Kosorygin VS. 2000. Experiments on receptivity, stability, and transition of two-dimensional laminar boundary layers with streamwise pressure gradients. See Fasel & Saric 2000, pp. 97–102
- Kosorygin VS, Polyakov NF. 1990. Autodestruction of unstable waves in a laminar boundary layer. *Preprint 11–90*, ITPM Akad. Nauk USSR Sib. Otd., Novosibirsk
- Kosorygin VS, Levchenko VYa, Polyakov NF. 1988. The laminar boundary layer in the presence of moderately turbulent freestream. *Preprint 16–88*, ITPM Akad. Nauk USSR Sib. Otd., Novosibirsk
- Kosorygin VS, Radeztsky RH Jr, Saric WS. 1995. Laminar boundary layer sound receptivity and control. See Kobayashi 1995, pp. 517–24
- Landahl MT. 1980. A note on an algebraic instability of inviscid parallel shear flows. *J. Fluid Mech.* 98:243–51
- Lin N, Reed HL, Saric WS. 1992. Effect of leading-edge geometry on boundary-layer receptivity to freestream sound. See Hussaini et al. 1992, pp. 421–40
- Luchini P. 2000. Reynolds number independent instability of the boundary layer over

- a flat surface: optimal perturbations. *J. Fluid Mech.* 404:289–309
- Mack LM. 1984. Boundary-layer linear stability theory. Special course on stability and transition of laminar flows. AGARD Rep. 709
- Matsubara M, Alfredsson PH. 2001. Disturbance growth in boundary layers subjected to freestream turbulence. *J. Fluid Mech.* 430:149–68
- Morkovin MV. 1969. On the many faces of transition. In *Viscous Drag Reduction*, ed. CS Wells, pp. 1–31. New York: Plenum
- Morkovin MV. 1993. Bypass-transition research: issues and philosophy. *Instabilities and Turbulence in Engineering Flows*, ed. DE Ashpis, TB Gatski, R Hirsh, pp. 3–30. Amsterdam: Kluwer
- Morkovin MV, Reshotko E, Herbert T. 1994. Transition in open flow systems—a reassessment. *Bull. Am. Phys. Soc.* 39:1882
- Nayfeh AH, Ashour ON. 1994. Acoustic receptivity of a boundary layer to Tollmien-Schlichting waves resulting from a finite-height hump at finite Reynolds numbers. *Phys. Fluids A* 6:3705–16
- Nishioka M, Morkovin MV. 1986. Boundary-layer receptivity to unsteady pressure gradients. *J. Fluid Mech.* 171:219–61
- Parekh DE, Pulvin P, Wlezien RW. 1991. Boundary-layer receptivity to convected gusts and sound. See Reda et al. 1991, pp. 69–76
- Reda DC, Reed HL, Kobayashi R, eds. 1991. *Boundary Layer Stability and Transition to Turbulence FED-114*. New York: ASME. 225 pp.
- Reed HL. 1994. Direct numerical simulation of transition: the spatial approach. See Saric 1994b, pp. 6.1–46
- Reed HL, Haynes TS, Saric WS. 1998. CFD validation issues in transition modeling. *AIAA J.* 36:742–51
- Reed HL, Saric WS, Arnal D. 1996. Linear stability theory applied to boundary layers. *Annu. Rev. Fluid Mech.* 28:389–428
- Reshotko E. 1976. Boundary-layer stability and transition. *Annu. Rev. Fluid Mech.* 8:311–49
- Reshotko E. 1984. Disturbances in a laminar boundary layer due to distributed surface roughness. See Tatsumi 1984, pp. 39–46
- Reshotko E. 1994. Boundary-layer instability, transition, and control. *AIAA Pap. 94-0001*
- Reshotko E. 1997. Progress, accomplishments and issues in transition research. *AIAA Pap. 97-1815*
- Reshotko E. 2001. Transient growth: a factor in bypass transition. *Phys. Fluids* 13:1067–75
- Saric WS, ed. 1994a. *Progress in Transition Modelling, AGARD Report 793*. Paris: NATO. 276 pp.
- Saric WS. 1994b. Physical description of boundary-layer transition: experimental evidence. See Saric 1994a, pp. 1.1–51
- Saric WS, Hoos JA, Radeztsky RH Jr. 1991. Boundary-layer receptivity of sound with roughness. See Reda et al. 1991, pp. 69–76
- Saric WS, Thomas ASW. 1984. Experiments on the subharmonic route to turbulence in boundary layers. See Tatsumi 1984, pp. 117–22
- Saric WS, Reed HL, Kerschen EJ. 1994. Leading edge receptivity to sound: experiments, DNS, and theory. *AIAA Pap. 94-2222*
- Saric WS, Wei W, Rasmussen BK, Krutckoff TK. 1995. Experiments on leading-edge receptivity to sound. *AIAA Pap. 95-2253*
- Saric WS, White EB. 1998. Influence of high-amplitude noise on boundary-layer transition to turbulence. *AIAA Pap. 98-2645*
- Saric WS, Reed HL, White EB. 1999. Boundary-layer receptivity to freestream disturbances and its role in transition. *AIAA Pap. 99-3788*
- Schmid PJ, Henningson DS. 2001. *Stability and Transition in Shear Flows*. New York: Springer
- Singer BA, Reed HL, Ferziger JH. 1989. Effect of streamwise vortices on transition in plane channel flow. *Phys. Fluids A* 1:1960–71
- Spencer SA, Saric WS, Radeztsky RH Jr. 1991. Boundary-layer receptivity: freestream sound with three-dimensional roughness. *Bull. Am. Phys. Soc.* 36:2618
- Su YC, Herbert T. 2000. Receptivity to

- freestream turbulence and the effect of longitudinal vortices in boundary-layer transition. See Fasel & Saric 2000, pp. 117–24
- Suder K, O'Brien J, Reshotko E. 1988. Experimental study of bypass transition in a boundary layer. *NASA-TM-100913*
- Tadjfar M, Bodonyi RJ. 1992. Receptivity of a laminar boundary layer to the interaction of a three-dimensional roughness element with time-harmonic freestream disturbances. *J. Fluid Mech.* 242:701–20
- Tatsumi T, ed. 1984. *Turbulence and Chaotic Phenomena in Fluids*. Amsterdam: Elsevier. 556 pp.
- Ustinov MV, Kogan MN, Skumilkin VG, Zhigulev SG. 2000. Experimental study of flat-plate boundary-layer receptivity to vorticity normal to leading edge. See Fasel & Saric 2000, pp. 137–42
- Wanderly JBV, Corke TC. 2001. Boundary-layer receptivity to freestream sound on elliptic leading edges of flat plates. *J. Fluid Mech.* 429:1–29
- Westin KJA, Bakchinov AA, Kozlov VV, Alfredsson PH. 1998. Experiments on localized disturbances in a flat-plate boundary layer. Part I: the receptivity and evolution of a localized freestream disturbance. *Eur. J. Mech. B Fluids* 17:823–46
- Westin KJA, Boiko AV, Klingmann BGB, Kozlov VV, Alfredsson PH. 1994. Experiments in a boundary layer subject to freestream turbulence. Part I: boundary-layer structure and receptivity. *J. Fluid Mech.* 281:193–218
- White EB, Saric WS, Radeztsky RH Jr. 2000. Leading-edge acoustic receptivity measurements using a pulsed-sound technique. See Fasel & Saric 2000, pp. 103–10
- Wiegel M, Wlezien RW. 1993. Acoustic receptivity of laminar boundary layers over wavy walls. *AIAA Pap.* 93–3280
- Wlezien RW. 1989. Measurement of boundary-layer receptivity at suction surfaces. *AIAA Pap.* 89–1006
- Wlezien RW. 1994. Measurement of acoustic receptivity. *AIAA Pap.* 94–2221
- Wlezien RW, Parekh DE, Island TC. 1990. Measurement of acoustic receptivity at leading edges and porous strips. *Appl. Mech. Rev.* 43 (Pt. 2): S167–74